

Safe and Smooth: Certified Continuous-Time Range-Only Localization

Frederike Dümbgen Connor Holmes Timothy D. Barfoot

Abstract—A common approach to localize a mobile robot is by measuring distances to points of known positions, called anchors. Locating a device from distance measurements is typically phrased as a non-convex optimization problem, stemming from the nonlinearity of the measurement model. Non-convex optimization problems may yield suboptimal solutions when local iterative solvers such as Gauss-Newton are employed. In this paper, we design an optimality certificate for continuous-time range-only localization. Our formulation allows for the integration of a motion prior, which ensures smoothness of the solution and is crucial for localizing from only a few distance measurements. The proposed certificate comes at little additional cost since it has the same complexity as the sparse local solver itself: linear in the number of positions. We show, both in simulation and on real-world datasets, that the efficient local solver often finds the globally optimal solution (confirmed by our certificate) and when it does not, simple random reinitialization eventually leads to the certifiable optimum.

Index Terms—certifiable algorithms, global optimality, Lagrangian duality, range-only localization

I. INTRODUCTION

Localizing a moving robot is an essential component of many real-world applications. One common approach to localization is to measure the distances to a certain number of fixed points, also called anchors. In mobile indoor localization, for instance, a phone can be localized by inferring distances to WiFi access points from time of flight or received signal strength of emitted pulses [1]. As another example, designated anchors equipped with the Ultra Wideband (UWB) technology may be employed for localization. This way, autonomous lawnmowers may accurately find their way in large grassy fields, where other approaches such as feature-based computer vision are compromised [2]. UWB has also become increasingly popular for the localization of robots in Global Positioning System (GPS)-denied areas, to enable, for instance, swarming or other forms of collaboration [3]. In all these examples, the locations of the anchors are known *a priori*, or can be estimated in a separate procedure [4]. The remaining task is to determine a moving device’s trajectory based on distance measurements, which is a form of multilateration.

Although multilateration is a standard problem, many important open questions persist. For instance, when approached from a robotics point of view, multilateration is called range-only localization and typically involves solving a nonlinear

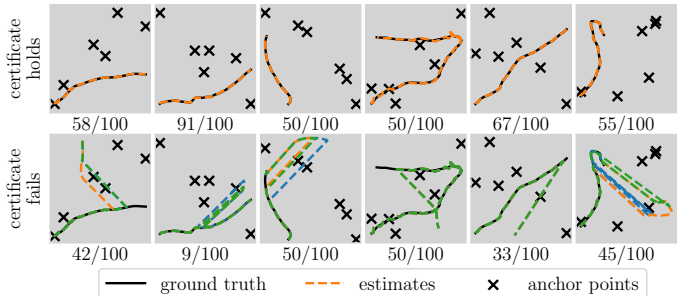


Fig. 1: Visualization of suboptimal solutions found by a local Gauss-Newton (GN) solver in range-only continuous-time localization. Solid lines corresponds to ground truth trajectories and the dashed coloured lines to estimates from various random initializations. Out of 100 random initializations, the 6 shown examples yield, for a high proportion of initializations (see labels below each plot), suboptimal solutions. The proposed method allows to identify such suboptimal solutions with little additional computational cost.

least-squares optimization problem. However, the available efficient solvers are only ensured to find local minima [5]. A more classical approach to multilateration is to exploit principles from distance geometry [6]. However, optimality and recovery guarantees obtained this way usually remain limited to the case where exact (noiseless) distances are given, and when a unique solution exists [7], [8]. Figure 1 displays the limitation of existing methods. In the shown examples, a moving device is localized based on distance measurements only. The distance measurements are noisy, and at each time, we only measure one distance; these factors rule out optimal solvers from distance geometry. We can solve the localization problem by phrasing it as a batch continuous-time range-only localization problem instead. However, as the examples in Figure 1 show, it is not uncommon for such a method to yield a suboptimal solution.

The method presented in this paper allows us to confirm when an optimal solution has been found. We first derive a certificate for discrete range-only localization without between-point dependencies. Although a novel contribution by itself, this certificate is not usually necessary, since the problem can be solved pointwise with efficient globally optimal solvers [9], [10]. However, such solvers do not allow for enforcing smoothness and are limited to scenarios where each sub-problem is well-determined. We extend the certificate to continuous-time range-only localization, which addresses both points, and for which no optimal solvers are known to this date. Our smoothness priors are enforced by regularization terms that stem from Gaussian Process (GP) regression and allow us to incorporate physical assumptions about the trajectory. As a

*This work was supported by the Swiss National Science Foundation, Postdoc Mobility grant number 206954.

All authors are with the Autonomous Space Robotics Lab, University of Toronto, Canada.

Corresponding author: frederike.dumbgen@utoronto.ca

welcome side effect, such a model can be used, for instance, to evaluate the trajectory at interpolated times, or to obtain closed-form estimates of quantities of interest such as the instantaneous velocity [11]. The proposed certificates show that local solvers yield the optimal solution in the vast majority of cases. More specifically, the contributions of this paper are:

- Certificates for multilateration and range-only continuous-time localization,
- a detailed treatment of how to exploit sparsity to compute the certificates in linear complexity, and
- validation of the proposed certificates, including evaluation on real-world datasets.

This paper is organized as follows. After reviewing related work in Section II, we introduce the certificate for multilateration and continuous-time range-only localization in Sections III-B and III-C, respectively. We include a discussion of our local solver in Section III-D and the certificate computation in Section III-E, both of which exploit the sparsity of the problem. We evaluate the certificates in simulation and on UWB-based drone localization experiments in Section IV, and conclude in Section V.

II. RELATED WORK

Range-only localization The underdetermined nature of distance measurements makes range-only localization (and its extension, range-only Simultaneous Localization and Mapping (SLAM)) a challenging subclass of state estimation problems. To account for the multi-modal distribution stemming from underdetermined measurements, prior work has focused on using Gaussian mixture models [12], [13] or sample-based models [14], [15] to approximate the position distribution in a filtering-inspired framework. More accurate than filters are batch solutions, which typically provide the maximum a posteriori (MAP) estimate of the trajectory given all measurements within a given time window [16]. A priori, batch solutions are more expensive than filtering, but the sparsity of the underlying measurement graph typically allows for efficient and incremental sparse solvers [17], [18]. In both batch and filter approaches, continuous-time rather than discrete-time trajectory models have been explored [16], through which smoothness can be incorporated, thereby helping with underdetermined measurements. To make the continuous-time estimation tractable, some prior work uses parametric representations with carefully chosen temporal basis functions [19], [20]. A popular alternative is non-parametric GP regression, which is easier to tune and has an elegant connection with physically plausible motion priors [11].

Whatever representation is used, at the core of batch MAP estimation is the solution of a non-convex minimization problem [16]. The latter is most commonly solved with an iterative minimizer, which provably converges to a stationary point, but not necessarily to the global minimum [5]. A different approach originated in the sensor network localization literature and studies the semi-definite relaxation of the optimization problem [21], [22]. However, optimality guarantees only exist for the noiseless case [7], and this approach scales poorly with batch size. Similarly, works inspired by distance geometry can

be exploited to recover both locations of anchor and trajectory points from between-point distance measurements. Tutorials of the topic are given in [6], [23] but, again, efficient algorithms with recovery guarantees only exist for scenarios that are too restrictive for robotics, such as the noiseless case [8].

With the proposed solution, we can be both efficient and optimal: we use a continuous-time batch approach, but exploit sparsity to keep the cost low enough for online inference, both in solving and certifying the solution. We place no assumptions on noise or uniqueness of the solution – as long as the certificate holds, the solution is optimal. Using the proposed certificate, we show that the efficient nonlinear solver almost always converges to the global optimum.

Optimality certificates In the last 10 years, significant progress was made in certifying solutions of common optimization problems in robotics and related fields. Certificates typically originate from Lagrangian duality principles [24], and were primarily introduced to robotics and computer vision for the problems of pose-graph optimization [25], [26] and rotation averaging [27]. The main difficulty of these problems stems from the non-convex constraints that emerge when estimating rotations. Existing provably optimal solvers require the solution of a Semi-Definite Program (SDP), which extends poorly to large batch sizes. Instead, follow-up works have investigated careful reformulation [28], Riemannian optimization [29], coordinate block descent [30], and an adaptation of, for instance, GN [31], to speed up the certified solvers. In parallel strands of research, significant progress has been made on using outlier-robust cost functions for optimal line fitting [32] and optimal point-cloud alignment [33], [34], respectively.

None of the above frameworks can be applied to the important class of problems where only distance measurements are available. The present paper aims to fill this gap. We follow the trend of avoiding the need to solve a large SDP, and instead provide an optimality certificate for a locally optimal solution obtained through an efficient iterative solver.

III. METHOD

A. Problem Statement and Notation

Our goal is to solve for an unknown state vector over time, which we denote by $\theta(t) \in \mathbb{R}^K$ at time t . The state typically contains the robot's position $x(t) \in \mathbb{R}^D$, with D typically 2 or 3 and $K \geq D$. As we see later, extending the state to include, for instance, the velocity, gives us more flexibility for imposing physically plausible priors. At certain known times $t_n, n = 1 \dots N$, we obtain distance measurements d_{mn} from the position $x_n := x(t_n)$ to known anchors $y_m \in \mathbb{R}^D, m = 1 \dots M$. By abuse of notation, we allow the number of observed anchors from each position to change, and we enumerate them as 1 to M_n , the number of observed anchors at position n . Therefore, the measurement model is

$$d_n = h_n(\theta(t_n)) = \begin{bmatrix} \|y_1 - x_n\|^2 \\ \vdots \\ \|y_{M_n} - x_n\|^2 \end{bmatrix} + n_n \in \mathbb{R}^{M_n}, \quad (1)$$

with $n_n \sim \mathcal{N}(\mathbf{0}, \Sigma_n)$ Gaussian measurement noise. We introduce the matrix of known anchor coordinates $Y_n =$

$[\mathbf{y}_1 \dots \mathbf{y}_{M_n}] \in \mathbb{R}^{D \times M_n}$ and the vector of its squared norms $\boldsymbol{\gamma}_n^\top = [\|\mathbf{y}_1\|^2 \dots \|\mathbf{y}_{M_n}\|^2] \in \mathbb{R}^{M_n}$. We introduce \mathbf{I}_d and $\mathbf{1}_d$ for the d -dimensional identity matrix and the vector of all ones, respectively, and \mathbf{i}_n^d for the length- d selection vector with a one at index n . Finally, we introduce time-concatenated vectors $\mathbf{x}^\top = [\mathbf{x}_1^\top \dots \mathbf{x}_N^\top]$, and $\text{Diag}(\mathbf{A}_n)_{n=1}^N$, the block-diagonal matrix composed of elements \mathbf{A}_n .

B. Certified Multilateration

We first derive a certificate for range-only localization without imposing any smoothness on the trajectory. Therefore, we assume that our state is discrete and consists only of the position: $\theta(t_n) = \mathbf{x}_n \in \mathbb{R}^D$. The problem could be separated into N smaller problems, each of which has an optimal solution [9], [10], but treating it jointly serves as a convenient starting point for the continuous-time certificates.

a) *Problem statement:* The MAP estimate can be obtained by solving

$$\hat{\theta} = \min_{\theta} f(\theta) = \min_{\theta} \sum_n \mathbf{e}_n^\top \Sigma_n^{-1} \mathbf{e}_n, \quad (2)$$

with $\mathbf{e}_n = \mathbf{d}_n - \mathbf{h}_n(\theta_n)$. Expanding row m of the error vector \mathbf{e}_n yields

$$\begin{aligned} e_{mn} &= d_{mn}^2 - \|\mathbf{y}_m - \mathbf{x}_n\|^2 \\ &= d_{mn}^2 - \|\mathbf{y}_m\|^2 + 2\mathbf{y}_m^\top \mathbf{x}_n - \|\mathbf{x}_n\|^2, \end{aligned} \quad (3)$$

which shows that (2) is a quartic function in the unknown vectors \mathbf{x}_n . To turn it into a quadratic function, we substitute $z_n = \|\mathbf{x}_n\|^2$. Then, introducing $\mathbf{f}_n^\top := [\mathbf{x}_n^\top \ z_n]$ and $\mathbf{b}_n := \mathbf{d}_n - \boldsymbol{\gamma}_n$ we can rewrite the error vector as $\mathbf{e}_n = \mathbf{Q}_n \mathbf{f}_n + \mathbf{b}_n$ and the substitution as $\mathbf{f}_n^\top \bar{\mathbf{A}} \mathbf{f}_n = 0$, with

$$\bar{\mathbf{A}} := \begin{bmatrix} \mathbf{I}_d & -\frac{1}{2} \\ -\frac{1}{2} & 0 \end{bmatrix}, \quad \mathbf{Q}_n := [2\mathbf{Y}_n^\top \ -1]. \quad (4)$$

Using above, we obtain the following Quadratically Constrained Quadratic Program (QCQP), equivalent to (2):

$$\begin{aligned} \min_{\mathbf{f}_n, n=1 \dots N} \ & \sum_n (\mathbf{Q}_n^\top \mathbf{f}_n + \mathbf{b}_n)^\top \Sigma_n^{-1} (\mathbf{Q}_n^\top \mathbf{f}_n + \mathbf{b}_n) \\ \text{s.t.} \ & \mathbf{f}_n^\top \bar{\mathbf{A}} \mathbf{f}_n = 0 \quad n = 1 \dots N, \end{aligned} \quad (5)$$

where the constraint enforces the substitution. Introducing $\mathbf{f} \in \mathbb{R}^F$, the vector of stacked variables of size $F = N(D+1)+1$,

$$\mathbf{f}^\top = [\mathbf{x}_1^\top \ z_1 \ \dots \ \mathbf{x}_N^\top \ z_N \ \ell], \quad (6)$$

with ℓ a homogenization variable, we can convert (5) into the standard, homogeneous QCQP:

$$\begin{aligned} (Q) \quad q^* &= \min_{\mathbf{f}} \mathbf{f}^\top \mathbf{Q} \mathbf{f} \\ \text{s.t.} \ & \mathbf{f}^\top \mathbf{A}_n \mathbf{f} = 0 \quad n = 1 \dots N \\ & \mathbf{f}^\top \mathbf{A}_0 \mathbf{f} = 1, \end{aligned} \quad (7)$$

with the matrices \mathbf{A}_n , \mathbf{A}_0 , and $\mathbf{Q} \in \mathbb{R}^{F \times F}$ given by

$$\mathbf{A}_n = \mathbf{S}_n \bar{\mathbf{A}} \mathbf{S}_n^\top, \quad \mathbf{S}_n = \begin{bmatrix} \mathbf{i}_n^N \otimes \mathbf{I}_{d+1} \\ \mathbf{0}^\top \end{bmatrix}, \quad \mathbf{A}_0 = \mathbf{i}_F^F \mathbf{i}_F^{F^\top},$$

$$\begin{aligned} \mathbf{Q} &= \begin{bmatrix} \mathbf{Q}_{11} & \dots & \mathbf{0} & \mathbf{q}_1 \\ \vdots & \ddots & \vdots & \vdots \\ \mathbf{0} & \dots & \mathbf{Q}_{NN} & \mathbf{q}_N \\ \mathbf{q}_1^\top & \dots & \mathbf{q}_N^\top & q_0 \end{bmatrix}, \quad q_0 = \sum_n \mathbf{b}_n^\top \Sigma_n^{-1} \mathbf{b}_n, \\ \mathbf{Q}_{nn} &= \begin{bmatrix} 4\mathbf{Y}_n \Sigma_n^{-1} \mathbf{Y}_n^\top & -2\mathbf{Y}_n \Sigma_n^{-1} \mathbf{1} \\ -2\mathbf{1}^\top \Sigma_n^{-1} \mathbf{Y}_n^\top & \mathbf{1}^\top \Sigma_n^{-1} \mathbf{1} \end{bmatrix}, \quad \mathbf{q}_n = \begin{bmatrix} 2\mathbf{Y}_n \Sigma_n^{-1} \mathbf{b}_n \\ -\mathbf{1}^\top \Sigma_n^{-1} \mathbf{b}_n \end{bmatrix}. \end{aligned}$$

We turn this problem into a SDP by introducing $\mathbf{F} = \mathbf{f} \mathbf{f}^\top$ (which is equivalent to $\mathbf{F} \succeq 0$, $\text{rank } \mathbf{F} = 1$) and relaxing the rank constraint. This gives the standard SDP relaxation of (Q), which we denote as the primal problem (P):

$$\begin{aligned} (P) \quad p^* &= \min_{\mathbf{F}} \text{tr}(\mathbf{Q}^\top \mathbf{F}) \\ \text{s.t.} \quad & \text{tr}(\mathbf{A}_n \mathbf{F}) = 0 \quad n = 1 \dots N \\ & \text{tr}(\mathbf{A}_0 \mathbf{F}) = 1 \\ & \mathbf{F} \succeq 0. \end{aligned} \quad (8)$$

The dual problem is given by

$$\begin{aligned} (D) \quad d^* &= \max_{\rho, \boldsymbol{\lambda}} (-\rho) \\ \text{s.t.} \quad & \mathbf{H}(\rho, \boldsymbol{\lambda}) := \mathbf{Q} + \sum_n \lambda_n \mathbf{A}_n + \rho \mathbf{A}_0 \succeq 0, \end{aligned} \quad (9)$$

where ρ and $\boldsymbol{\lambda}^\top = [\lambda_1 \dots \lambda_N] \in \mathbb{R}^N$ are the dual variables.

At this point, it is useful to take a step back and consider what we have achieved so far. We have relaxed our original nonlinear state estimation into a standard SDP. Now, we could take at least two different approaches to solving the original problem:

- Solve the relaxed problem (P), and investigate the solution, denoted by \mathbf{F}^* . If the obtained solution has rank 1, then we can decompose it into $\mathbf{F}^* = \mathbf{f}^* \mathbf{f}^{*\top}$ (using, for instance, an Eigenvalue Decomposition (EVD)), where \mathbf{f}^* is exactly the globally optimal solution to (Q).
- Solve the primal problem (Q) locally using an iterative nonlinear solver. This will return a solution that is ensured to be locally optimal; we call this estimate $\hat{\mathbf{f}}$. Then, we can use optimality conditions from duality theory to derive a certificate for this solution: if the certificate holds, the solution is in fact optimal and we have $\hat{\mathbf{f}} = \mathbf{f}^*$.

In this paper, we take the second approach. This choice is motivated by two observations. First, in standard localization problems, we aim to solve for a large number of points simultaneously, yielding a large SDP for (P). The typical complexity of available solvers is cubic in the number of points [5], making them too slow for real-time robotics applications. Second, we found that even a basic iterative solver often converges to the optimal solution, in particular for the noise levels that are adequate for localization problems. As we will show, such solvers can exploit the sparsity of the problem in a principled manner, which makes them significantly faster than SDP solvers.

b) *Certificate:* Our aim is to determine whether a locally optimal solution $\hat{\mathbf{f}}$ is also the global optimum. We obtain a local solution $\hat{\mathbf{x}}$ from a standard iterative GN solver, as outlined in III-D, and augment it to $\hat{\mathbf{f}}$ as in (6). We know

from duality theory (see *e.g.*, [35]) that if we can find dual variables $\hat{\rho}, \hat{\lambda}$ such that:

$$\hat{\mathbf{f}}^\top \mathbf{A}_0 \hat{\mathbf{f}} = 1, (\forall n) \hat{\mathbf{f}}^\top \mathbf{A}_n \hat{\mathbf{f}} = 0 \text{ (primal feasibility)} \quad (10)$$

$$\mathbf{H}(\hat{\rho}, \hat{\lambda}) \succeq 0 \text{ (dual feasibility)} \quad (11)$$

$$\mathbf{H}(\hat{\rho}, \hat{\lambda}) \hat{\mathbf{f}} = \mathbf{0} \text{ (stationarity condition)} \quad (12)$$

then $\hat{\mathbf{f}}$ (and thus $\hat{\mathbf{x}}$) is in fact the optimal solution to (Q). Note that the conditions are sufficient, but not necessary – if a solution does not satisfy all conditions it may still be an optimal solution. However, in our experiments, this case never occurred (see Section IV-A). Because $\mathbf{H}(\hat{\rho}, \hat{\lambda})$ plays such a crucial role, we will refer to it as the ‘certificate matrix’.

The primal feasibility is trivial by construction, so we only need to verify the last two conditions. We can rewrite the stationarity condition as

$$\mathbf{Ly} := [\mathbf{A}_1 \hat{\mathbf{f}} \dots \mathbf{A}_N \hat{\mathbf{f}} \mathbf{A}_0 \hat{\mathbf{f}}] \hat{\mathbf{y}} = -\mathbf{Q} \hat{\mathbf{f}} := \mathbf{b}, \quad (13)$$

with $\hat{\mathbf{y}} := [\hat{\lambda}_1 \dots \hat{\lambda}_N \hat{\rho}]^\top$, which is a linear system with K equations and $N+1$ unknowns, and a priori, may not have a solution. However, as we see next, some of the equations are redundant and the system of equations admits a single unique solution. Plugging the expressions for \mathbf{Q} , \mathbf{A}_i , and $\hat{\mathbf{f}}$ in (13), the N equations corresponding to the substitution variables (rows $n+1$, $n = 1 \dots N$) take the form

$$(\forall n) -\frac{1}{2} \hat{\lambda}_n = -\mathbf{1}^\top \Sigma_n^{-1} \mathbf{e}_n, \quad (14)$$

which can be solved for $\hat{\lambda}_n$. Plugging the solution into the other ND rows involving $\hat{\lambda}_n$, we need to show that

$$(\forall n) \hat{\mathbf{x}}_n \hat{\lambda}_n = 2\hat{\mathbf{x}}_n \mathbf{1}^\top \Sigma_n^{-1} \mathbf{e}_n \stackrel{?}{=} 2\mathbf{Y}_n \Sigma_n^{-1} \mathbf{e}_n, \quad (15)$$

or in other words, we need these equations to be redundant. We can show that (15) indeed holds because $\hat{\mathbf{x}}_n$ are stationary points of (2) and thus

$$(\forall n) \nabla_{\mathbf{x}_n} f = 4(\mathbf{Y}_n - \hat{\mathbf{x}}_n \mathbf{1}^\top) \Sigma_n^{-1} \mathbf{e}_n = \mathbf{0}. \quad (16)$$

Finally, we can use (16) and the last line of (13) to solve for $\hat{\rho}$, which gives

$$\begin{aligned} \hat{\rho} &= -\sum_n \frac{1}{2} \|\hat{\mathbf{x}}_n\|^2 \hat{\lambda}_n + 2\mathbf{b}^\top \Sigma_n^{-1} \mathbf{e}_n \\ &= -\sum_n \left(\|\hat{\mathbf{x}}_n\|^2 \mathbf{1}^\top + 2\mathbf{b}^\top \right) \Sigma_n^{-1} \mathbf{e}_n \\ &= -\sum_n \left(\mathbf{e}_n^\top - 2\mathbf{x}_n^\top \mathbf{Y}_n + 2\|\hat{\mathbf{x}}_n\|^2 \mathbf{1}^\top \right) \Sigma_n^{-1} \mathbf{e}_n \\ &= -\sum_n \mathbf{e}_n^\top \Sigma_n^{-1} \mathbf{e}_n - 2\mathbf{x}_n^\top (\mathbf{Y}_n - \hat{\mathbf{x}}_n \mathbf{1}^\top) \Sigma_n^{-1} \mathbf{e}_n \\ &= -\sum_n \mathbf{e}_n^\top \Sigma_n^{-1} \mathbf{e}_n. \end{aligned} \quad (17)$$

Note that the analytical solution of $\hat{\rho}$ shows that strong duality holds between (Q) and (D), as we have $d^* = -\hat{\rho} = p^*$, provided (11) holds.

In summary, given a locally optimal solution $\hat{\mathbf{f}}$, we can use (14) and (17) to solve for the optimal dual variables. If they are such that the certificate matrix is positive-semidefinite (PSD), all conditions (10) to (12) are satisfied and we conclude that $\hat{\mathbf{f}}$ is in fact the optimal solution to (P).

C. Certified Continuous-Time Range-Only Localization

The previous example has taught us how to certify the optimality of a candidate solution to the range-only localization problem. However, we reiterate that efficient optimal solvers for problem (2) exist, therefore locally solving and then certifying the solution is not justified in general.

However, we can use what we have learned to extend the method to incorporate motion priors, a case for which no efficient, provably optimal solvers are known. The certificates developed hereafter allow us to use a local solver, followed by a certificate check, both of which can be implemented efficiently by exploiting sparsity. As we will see in Section IV, the fast local solver finds the global optimum most of the time, and suboptimal solutions can be avoided through simple reinitialization; our certificate can tell us when this is necessary.

a) Motion Prior: Since robots move according to physical laws, the resulting trajectories typically exhibit a certain degree of smoothness. A principled way to formalize this fact is by expressing the trajectory as a GP, with a one-to-one correspondence between both the covariance and mean functions and the assumed motion model, as described in more detail in [11]. In contrast with Section III-B, the state vector $\theta(t) \in \mathbb{R}^K$ may now consist of more states than just the position; for instance, we may add orientation and/or velocity. We assume that $\theta(t)$ is a GP:

$$\theta(t) \sim \mathcal{GP}(\mu(t), K(t, t')), \quad t_0 < t, t' \quad (18)$$

where $\mu(t)$ is the mean function, $K(t, t')$ is the covariance function between two times, and t_0 is the starting time. One particular class of covariance functions comes from modeling motion as a linear, time-varying (LTV) system, in which case the motion of the device can be described by

$$\dot{\theta}(t) = \mathbf{A}(t)\theta(t) + \mathbf{B}(t)\mathbf{u}(t) + \mathbf{F}(t)\mathbf{w}(t), \quad (19)$$

with $\mathbf{A}(t)$, $\mathbf{B}(t)$ and $\mathbf{F}(t)$ known system matrices, $\mathbf{u}(t)$ a known input and $\mathbf{w}(t) \sim \mathcal{GP}(\mathbf{0}, Q_C \delta(t - t'))$, a stationary zero-mean GP with power spectral density matrix Q_C . The general solution to this model is

$$\begin{aligned} \theta(t) &= \Phi(t, t_0)\theta(t_0) + \\ &\quad \int_{t_0}^t \Phi(t, s)(\mathbf{B}(s)\mathbf{u}(s) + \mathbf{F}(s)\mathbf{w}(s))ds, \end{aligned} \quad (20)$$

where $\Phi(t, t')$ is the transition function. To make the model more tangible, we introduce two example motion priors.

Example 1: zero-velocity prior By setting the state to the position only ($\theta(t) = \mathbf{x}(t)$), and the system matrices to $\mathbf{A}(t) = \mathbf{F}(t) = \mathbf{I}$, and $\mathbf{B}(t) = \mathbf{0}$, we obtain the ‘zero-velocity’ prior, meaning we assume that there is no motion between two consecutive points. In this case, the transition matrix is simply $\Phi(t, t') = \mathbf{I}$, and we obtain a regularization term equivalent to Tikhonov regularization.

Example 2: constant-velocity prior A more useful motion prior is generated by the constant-velocity assumption. It is obtained by setting:

$$\theta(t) = \begin{bmatrix} \mathbf{x}(t) \\ \mathbf{v}(t) \end{bmatrix}, \mathbf{A}(t) = \begin{bmatrix} \mathbf{0} & \mathbf{I} \\ \mathbf{0} & \mathbf{0} \end{bmatrix}, \mathbf{B}(t) = \mathbf{0}, \mathbf{F}(t) = \begin{bmatrix} \mathbf{0} \\ \mathbf{I} \end{bmatrix},$$

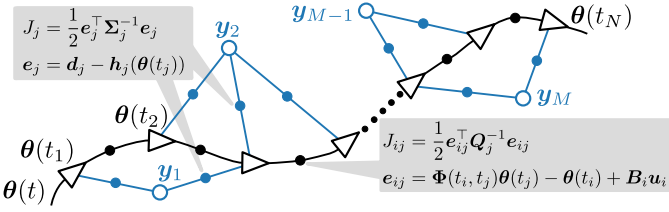


Fig. 2: Factor graph representation of the GP inference problem. Black factors represent the motion prior, blue are the range-only measurement factors.

where $v(t)$ denotes the velocity at time t . In this case, the transition matrix is

$$\Phi(t, t') = \begin{bmatrix} \mathbf{I} & (t - t')\mathbf{I} \\ \mathbf{0} & \mathbf{I} \end{bmatrix}. \quad (21)$$

Whatever the motion prior, the MAP estimate of the trajectory under the GP assumption and given the distance measurements, can be obtained by solving

$$\hat{\theta} = \min_{\theta} f(\theta) + r(\theta), \quad r(\theta) := \sum_{n=2}^N \mathbf{e}_{n,n-1} \mathbf{Q}_n^{-1} \mathbf{e}_{n,n-1}, \quad (22)$$

where $f(\theta)$ is as defined in (2), and we have introduced

$$\mathbf{e}_{n,n-1} := \Phi_{n,n-1} \theta_{n-1} - \theta_n + \mathbf{B}_n \mathbf{u}_n \quad (23)$$

$$\mathbf{u}_n := \int_{t_{n-1}}^{t_n} \Phi(t_n, s) \mathbf{B}(s) \mathbf{u}(s) ds \quad (24)$$

$$\mathbf{Q}_n := \int_{t_{n-1}}^{t_n} \Phi(t_n, s) \mathbf{F}(s) \mathbf{Q}_c \mathbf{F}(s)^\top \Phi(t_n, s)^\top ds, \quad (25)$$

and $\theta_n := \theta(t_n)$, $\mathbf{B}_n := \mathbf{B}(t_n)$, and $\Phi_{ij} := \Phi(t_i, t_j)$. The important point to note is that each regularization term in (22) depends only on the previous and subsequent position, owing to the Markov property. The inference problem is thus still sparse, which we will exploit later to develop efficient solvers. To visualize this point, we show in Figure 2 the factor-graph representation of the inference problem. The Gaussian prior results in state-to-state factors, taking a similar role as Inertial Measurement Unit (IMU) measurements would in classical SLAM problems.

Comparing (22) to (2), we have merely added the regularization term $r(\theta)$ to the cost function, which, as we show in the next section, does not significantly affect the derived certificates. Before moving on, we do a few manipulations to bring the new cost function into our standard form. First, we note that $r(\theta)$ can be written as $\theta^\top \mathbf{R} \theta$, where

$$\mathbf{R} = \begin{bmatrix} \mathbf{R}_1 \\ \mathbf{R}_2 \\ \vdots \\ \mathbf{R}_{N-1} \\ \mathbf{R}_N \end{bmatrix} = \begin{bmatrix} \mathbf{R}_{11} & \mathbf{R}_{12} & \mathbf{0} & \cdots & \mathbf{0} \\ \mathbf{R}_{12}^\top & \mathbf{R}_{22} & \mathbf{R}_{23} & \ddots & \vdots \\ \mathbf{0} & \ddots & \ddots & \ddots & \mathbf{0} \\ \vdots & \ddots & \ddots & \ddots & \mathbf{R}_{N-1,N} \\ \mathbf{0} & \cdots & \mathbf{0} & \mathbf{R}_{N-1,N}^\top & \mathbf{R}_{NN} \end{bmatrix},$$

with $\mathbf{R}_{n,n+1} = -\Phi_{n+1,n}^\top \mathbf{Q}_{n+1}^{-1}$ for $1 \leq n \leq N-1$ and

$$\mathbf{R}_{nn} = \begin{cases} \mathbf{Q}_n^{-1} + \Phi_{n+1,n}^\top \mathbf{Q}_{n+1}^{-1} \Phi_{n+1,n} & \text{for } 2 \leq n \leq N-1 \\ \Phi_{n+1,n}^\top \mathbf{Q}_{n+1}^{-1} \Phi_{n+1,n} & \text{for } n = 1 \\ \mathbf{Q}_n^{-1} & \text{for } n = N \end{cases}. \quad (26)$$

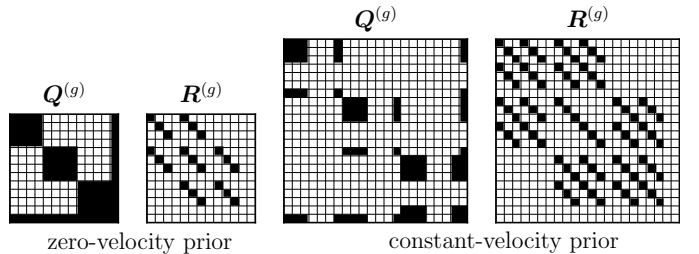


Fig. 3: Sparsity patterns of the cost matrices obtained using zero-velocity or constant velocity priors for $N = 4$.

We also introduce the new vector \mathbf{g} :

$$\mathbf{g}^\top = [\mathbf{g}_1^\top \ z_1 \ \dots \ \mathbf{g}_N^\top \ z_N \ 1], \quad (27)$$

where we do not add any substitution variables for the components of θ_n other than x_n because the added regularization is already quadratic in θ_n . We then augment \mathbf{R} with zero rows and columns where the regularization is zero (*i.e.*, for the substitution variables), yielding $\mathbf{R}^{(g)}$. Similarly, we create $\mathbf{Q}^{(g)}$ and $\mathbf{A}_i^{(g)}$, $i = 0 \dots N$ by padding with zeros for the variables in θ_n other than the position. Finally, we can write (22) in the standard form

$$\begin{aligned} (\text{Q-GP}) \quad q_{GP}^* = & \min_{\mathbf{g}} \mathbf{g}^\top \mathbf{Q}^{(g)} \mathbf{g} + \mathbf{g}^\top \mathbf{R}^{(g)} \mathbf{g} \\ \text{s.t. } & \mathbf{g}^\top \mathbf{A}_n^{(g)} \mathbf{g} = 0 \quad n = 1 \dots N \\ & \mathbf{g}^\top \mathbf{A}_0^{(g)} \mathbf{g} = 1. \end{aligned} \quad (28)$$

We show examples of the zero-padded cost matrices using the two different regularizations in Figure 3.

b) Certificate: Comparing (Q-GP) with (Q) it is clear that a new certificate can be derived by checking conditions (10) to (12), but with the new system matrices. In particular, we define the new certificate matrix

$$\mathbf{H}_{GP}(\hat{\rho}, \hat{\lambda}) = \mathbf{Q}^{(g)} + \mathbf{R}^{(g)} + \hat{\rho} \mathbf{A}_0^{(g)} + \sum_n \hat{\lambda}_n \mathbf{A}_n^{(g)}. \quad (29)$$

We note again that primal feasibility (10) is given by construction. The stationarity condition (12) now reads

$$[\mathbf{A}_1^{(g)} \hat{\mathbf{g}} \ \dots \ \mathbf{A}_N^{(g)} \hat{\mathbf{g}} \ \mathbf{A}_0^{(g)} \hat{\mathbf{g}}] \hat{\mathbf{y}} = -\mathbf{Q}^{(g)} \hat{\mathbf{g}} - \mathbf{R}^{(g)} \hat{\mathbf{g}}. \quad (30)$$

Note, however, that the matrix $\mathbf{R}^{(g)}$ is zero in the N rows and columns corresponding to the substitutions, and the corresponding lines of the left-hand side also remain unchanged. Therefore, we can still use (14) to solve for $\hat{\lambda}$, but we need to show that the remaining rows are redundant. For the sake of brevity, we provide a detailed treatment for the constant-velocity motion prior only. Equivalent results for other priors are a natural extension of this case (*i.e.*, eliminate \hat{v}_n for the zero-velocity prior, or replace it with other augmented state variables for other priors).

Example 2: We need to show that

$$(\forall n) \quad \hat{\theta}_n \hat{\lambda}_n = \begin{bmatrix} \hat{x}_n \\ \hat{v}_n \end{bmatrix} \hat{\lambda}_n \stackrel{?}{=} \begin{bmatrix} 2\mathbf{Y}_n \Sigma_n^{-1} \mathbf{e}_n \\ \mathbf{0} \end{bmatrix} + \begin{bmatrix} \mathbf{R}_{n,x} \\ \mathbf{R}_{n,v} \end{bmatrix} \hat{\theta}, \quad (31)$$

where $\mathbf{R}_{n,x}$ and $\mathbf{R}_{n,v}$ are the first D and remaining block-rows, respectively, of \mathbf{R}_n as defined in (26). Equations (31)

hold because $\hat{\theta}_n$ are stationary points of the cost function $f(\theta) + r(\theta)$ defined in (22), which means that

$$\mathbf{0} = \nabla_{\mathbf{x}_n} f(\hat{\theta}) + \nabla_{\mathbf{x}_n} r(\hat{\theta}) \quad (32)$$

$$= 4(\mathbf{Y}_n - \hat{\mathbf{x}}_n \mathbf{1}^\top) \Sigma_n^{-1} \mathbf{e}_n + \mathbf{R}_{n,x} \hat{\theta}, \quad (33)$$

$$\mathbf{0} = \nabla_{\mathbf{v}_n} r(\hat{\theta}) = \mathbf{R}_{n,v} \hat{\theta}. \quad (34)$$

Similarly, we start with the same expression for $\hat{\rho}$ as in (17), but this time, using (34), we obtain

$$\hat{\rho} = - \sum_n \mathbf{e}_n^\top \Sigma_n^{-1} \mathbf{e}_n - 2\hat{\mathbf{x}}_n^\top (\mathbf{Y}_n - \hat{\mathbf{x}}_n \mathbf{1}^\top) \Sigma_n^{-1} \mathbf{e}_n \quad (35)$$

$$= - \sum_n \mathbf{e}_n^\top \Sigma_n^{-1} \mathbf{e}_n - \sum_n \hat{\mathbf{x}}_n^\top \mathbf{R}_{n,x} \hat{\theta}. \quad (36)$$

Again, if the dual variables are feasible, then (36) implies strong duality provided that $\sum_n \hat{\mathbf{v}}_n^\top \mathbf{R}_{n,v} \hat{\theta} = \mathbf{0}$. This is the case thanks to (34).

D. Iterative Solver

The proposed certificate is applicable for any solution candidate satisfying first-order stationarity. A number of nonlinear least-squares solvers could be used to obtain such a candidate [5]. We give a brief outline of our implemented sparse GN solver, which we choose because of its wide usage and efficiency [16]. The GN iterates are $\theta^{k+1} = \theta^k + \delta\theta$, where each update $\delta\theta$ is calculated from

$$(\mathbf{R} + \mathbf{J}^\top \Sigma^{-1} \mathbf{J}) \delta\theta = \mathbf{R}(\mu - \theta^k) + \mathbf{J}^\top \Sigma^{-1} (\mathbf{y} - \mathbf{h}(\theta^k)). \quad (37)$$

Here, $\mathbf{J} := \text{Diag}(\nabla_{\mathbf{x}_n} \mathbf{h}_n)_{n=1}^N$ is the measurement Jacobian, and $\Sigma^{-1} := \text{Diag}(\Sigma_n^{-1})_{n=1}^N$. The vector μ contains the prior mean function and can be set to zero. Equation (37) is a sparse linear system of equations due to the form of the left-hand-side matrices, and can be solved efficiently via, for instance, sparse Cholesky factorization. The complexity of each iteration is thus $O(N)$ and we found that in practice, convergence was obtained after few (<10) iterations.

E. Efficient Certificate Computation

For a practical solution, we require not only an efficient iterative solver, but also an efficient certificate. Since we can solve analytically for the optimal dual variables in $O(N)$ time, the bottleneck of the computation lies in certifying PSD-ness of the certificate matrix, which is of size $N(K+1)+1$. The most intuitive approach of computing the eigenvalues of this matrix, is prohibitively expensive, with complexity of up to $O(N^3)$ [36]. Thankfully, we can exploit the particular sparsity pattern of the matrix to bring the cost of the certificate down to $O(N)$, as we will outline next.

The certificate matrix is a block-tridiagonal arrowhead matrix and belongs to the class of chordally sparse matrices, which exhibit numerous interesting properties (see [37] for an overview). The chordal property we exploit here is that the sparsity pattern is ‘preserved’ in the \mathbf{L} matrix of the \mathbf{LDL}^\top

decomposition. For our sparsity pattern, the certificate matrix is PSD, if and only if it can be decomposed as

$$\mathbf{H} = \mathbf{LDL}^\top, \quad \mathbf{D} = \text{Diag}([(D_n)_{n=1}^N, \delta]),$$

$$\mathbf{L} = \begin{bmatrix} \mathbf{J}_1 & \mathbf{0} & \cdots & \cdots & \mathbf{0} \\ \mathbf{L}_1 & \ddots & \ddots & & \vdots \\ \vdots & \ddots & \ddots & \ddots & \vdots \\ \mathbf{0} & \cdots & \mathbf{L}_{N-1} & \mathbf{J}_N & \mathbf{0} \\ \mathbf{l}_1^\top & \cdots & \mathbf{l}_{N-1}^\top & \mathbf{l}_N^\top & 1 \end{bmatrix}, \quad (38)$$

where \mathbf{J}_n are lower-diagonal matrices and \mathbf{D}_n are diagonal matrices with non-negative elements. \mathbf{L}_n and \mathbf{l}_n are a priori dense matrices and vectors, respectively. Equating the non-zero elements in (38) with the corresponding blocks of $\mathbf{H}(\hat{\rho}, \hat{\lambda})$, we obtain the following equalities:

$$\mathbf{H}_{nn} = \begin{cases} \mathbf{J}_n \mathbf{D}_n \mathbf{J}_n^\top & \text{for } n = 1 \\ \mathbf{L}_{n-1} \mathbf{D}_{n-1} \mathbf{L}_{n-1}^\top + \mathbf{J}_n \mathbf{D}_n \mathbf{J}_n^\top & \text{for } 2 \leq n \leq N \end{cases},$$

$$\mathbf{h}_n = \begin{cases} \mathbf{J}_n \mathbf{D}_n \mathbf{l}_n & \text{for } n = 1 \\ \mathbf{L}_{n-1} \mathbf{D}_{n-1} \mathbf{l}_{n-1} + \mathbf{J}_n \mathbf{D}_n \mathbf{l}_n & \text{for } 2 \leq n \leq N \end{cases},$$

$$\mathbf{H}_{n,n+1} = \mathbf{J}_n \mathbf{D}_n \mathbf{L}_n^\top \text{ for } 1 \leq n \leq N-1,$$

$$\mathbf{h} = \sum_{n=1}^N \mathbf{l}_n^\top \mathbf{D}_n \mathbf{l}_n + \delta. \quad (39)$$

These equations define a recursive scheme for computing the decomposition; the unknown factors can be computed in the order $\mathbf{D}_1, \mathbf{J}_1, \mathbf{L}_1, \dots, \mathbf{D}_N, \mathbf{J}_N, \mathbf{L}_N, \mathbf{l}_1 \dots \mathbf{l}_N, \delta$. The factors \mathbf{D}_n and \mathbf{J}_n are computed through individual \mathbf{LDL}^\top decompositions, but the involved matrices are only of size $K+1$. We can stop computing the decomposition early if we find a negative diagonal value, as the certificate has failed. The algorithm runs in $O(N)$ and as we show in simulation, has roughly the same absolute runtime as the GN solver.

IV. EXPERIMENTAL RESULTS

In this section, we show the effectiveness of the proposed method on simulated data and in real experiments. We give a detailed study of the performance of the certificate, showing that a local solver finds the optimal solution in a high proportion (about 95%) of random trials, and when it fails to do so, the certificate fails to hold, and a new solution can be generated by re-initializing, in which case we always find the global optimum eventually. Finally, we use our certificate to evaluate the localization performance in a real-world scenario with distance measurements from UWB anchors measured on a flying drone.

A. Simulation Results

a) Setup: We create simulated experiments as follows. We generate trajectories according to the constant-velocity model, where for each random instance we draw an initial velocity and position vector uniformly from $[-1, 1]$. The noise on the acceleration is set to $\sigma_v = 0.2$. The anchors are drawn uniformly at random from $[0, 1]$ and the bounding box is scaled to the size of the trajectory. We set $N = 100$, $M = 6$ and $D = 2$. We measure distances from all anchors at each time, and we generate measurements by adding Gaussian noise to

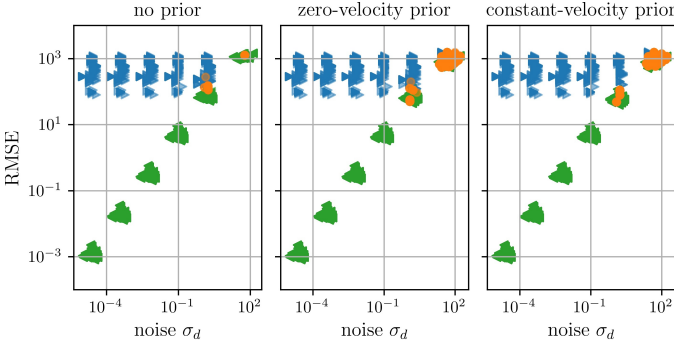


Fig. 4: Certificate value vs. root-mean-squared error (RMSE), using different motion priors obtained through simulations with $N = 100$, $M = 6$ and $D = 2$. The group of solutions corresponding to the smallest error out of 100 initializations are labelled optimal. The proposed certificate successfully labels all optimal solutions.

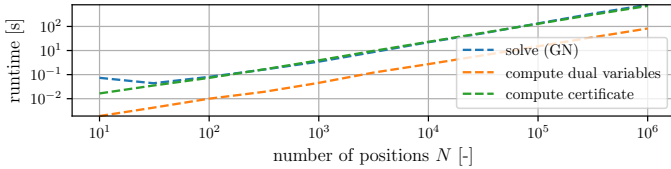


Fig. 5: Computation time of our GN solver, evaluating the dual variables, and computing the certificate, respectively, with increasing number of positions N .

the true distances before squaring them. We assume *i.i.d.* zero-mean noise with variance σ_d . For each random experimental setup, we solve using the GN algorithm, using 100 different random initializations, and using no prior, a zero-velocity prior and a constant-velocity prior, respectively. For simplicity, we set Σ_n^{-1} and Q_n^{-1} to the true values.

b) *Results:* We show qualitative results for noise level $\sigma_d = 10^{-3}$ in Figure 1. For most random setups and initializations, the solutions are close to the ground-truth trajectory, as shown in the first row of Figure 1. We label such solutions as globally optimal. Only for 6 out of 100 initializations (exactly the ones shown), certain initializations lead to local optima, depicted in the second row of Figure 1. The certificate correctly labels all optimal solutions, and fails for the local solutions.

We study the effect of noise in a quantitative analysis in Figure 4. We vary the distance noise σ_d and report the RMSE between the estimated and ground-truth trajectory. Since we lack an optimal solver, we label solutions as globally optimal when they correspond to (up to numerical tolerance) the smallest error for a given setup, and locally optimal otherwise. This method is reliable for small noise levels, as a big gap exists between the RMSE of the local and global solutions, but less so for higher noise. Most importantly, we observe that there are no false positives — the certificate never holds for a suboptimal solution. There are only few misses (false negatives), at the higher noise levels where our heuristic for labeling solutions may fail. Interestingly, we observe that although the certificate is only a sufficient condition in theory, it is effectively a necessary condition in practice: when the certificate does not hold, the solution always seems to be suboptimal.

We also study the computation time with increasing number

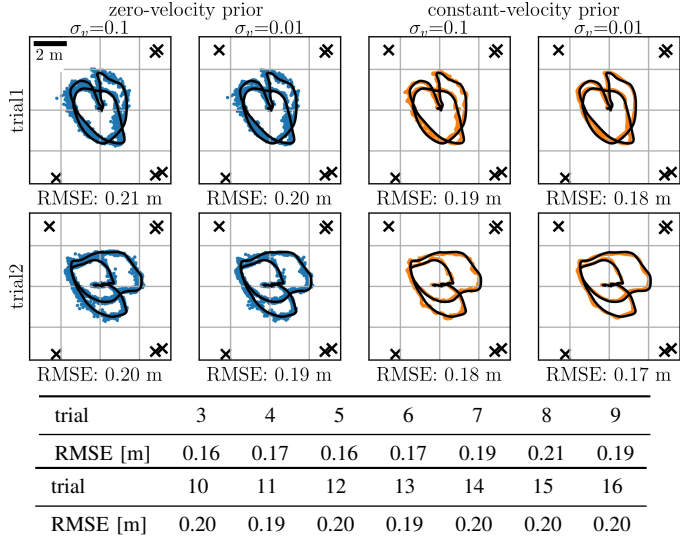


Fig. 6: Planar projections of certified solutions for two instances of the flying drone dataset, using the constant-velocity prior (blue) and the zero-velocity prior (orange), with varying parameter σ_v . The ground truth is shown in black. The tables below show the equally low RMSE for the certified solutions of the remaining trials, using the constant-velocity prior and $\sigma_v = 0.01$.

of positions N . Figure 5 shows that both the computation times of the solver and certificate increase linearly with N , and they are roughly equal. We run our method on up to a million positions, showing the scalability of this approach.

B. Experimental UWB Drone Dataset

Finally, we test the certificate on a dataset collected by a drone in a flying arena. There are $M = 6$ UWB anchors, placed in 6 corners of the flying arena, and measurements are obtained asynchronously, resulting in exactly one distance measurement at a time. Ground truth position is obtained with a Vicon motion capture setup. The setup is described in more detail in [38]. In total, 16 different flights (trials) with different trajectories are performed. The average measurement frequency per anchor is 5 Hz, and each trial being roughly one minute long, we obtain about $N = 2500$ measurement times for each trial.

Remarkably, our certificate tells us that the local solver finds the global solution in all 16 trials. We postulate that this is thanks to good anchor placement, as the suboptimal solutions in simulation were mostly observed for somewhat degenerate configurations. The planar projections of the estimated vs. ground-truth trajectories for two trials, using the two example motion priors, are shown in Figure 6, along with the RMSE values of all trials. Note that lower RMSE could be obtained by removing measurement bias or outliers [38]. The aim of this paper being optimality rather than accuracy, we do not perform any such preprocessing. Comparing the RMSE values across motion priors in Figure 6, we observe that the results with the constant-velocity prior are the most accurate, and that the parameter σ_v needs to be chosen carefully. Results without a motion prior are not shown because this would require heuristics such as interpolation, to have at least $D + 1$ at each time (required for each subproblem to

be well-determined). The proposed method circumvents this requirement without compromising optimality.

V. CONCLUSION AND FUTURE WORK

We have provided optimality certificates for range-only continuous-time localization. Distance measurements have been under-explored to this date in the related work on certified optimality, despite a wide range of applications. We have derived a closed-form solution for the optimal Lagrange multipliers that depends only on the residuals of the problem, and provided an efficient method for checking if the certificate matrix is PSD. We have successfully certified the solutions found by a sparsity-exploiting GN solver both in simulation and real experiments, and observed that the global optimum is found in most cases, in particular when the anchors are placed in non-degenerate configurations. The proposed certificate is an important first step to extend existing provably optimal solvers to range-only and other nonlinear measurements. A promising line of future work is the extension of the results to the full SLAM setup, where the anchor positions are unknown a priori. In a second step, the sparsity of the problem suggests that incorporating certificates into incremental solvers such as [18] could decrease the computational cost of the proposed method even further. Finally, the least-squares formulation used herein is sensitive to outliers, and could be replaced with a more robust cost function [34], [32].

ACKNOWLEDGMENTS

We would like to thank Abhishek Goudar of the Dynamic Systems Lab for providing us with the drone dataset.

REFERENCES

- [1] A. Raza, L. Lolic, S. Akhter, and M. Liut, “Comparing and Evaluating Indoor Positioning Techniques,” in *International Conference on Indoor Positioning and Indoor Navigation (IPIN)*, 2021.
- [2] J. Djugash, S. Singh, G. Kantor, and W. Zhang, “Range-only SLAM for robots operating cooperatively with sensor networks,” in *IEEE ICRA*, 2006, pp. 2078–2084.
- [3] W. Shule, C. M. Almansa, J. P. Queralta, Z. Zou, and T. Westerlund, “UWB-Based Localization for Multi-UAV Systems and Collaborative Heterogeneous Multi-Robot Systems,” *Procedia Computer Science*, vol. 175, pp. 357–364, 2020.
- [4] M. Hamer and R. D’Andrea, “Self-Calibrating Ultra-Wideband Network Supporting Multi-Robot Localization,” *IEEE Access*, vol. 6, pp. 22 292–22 304, 2018.
- [5] J. Nocedal and S. J. Wright, *Numerical Optimization*, ser. Springer Series in Operations Research. New York: Springer-Verlag, 1999.
- [6] L. Liberti, C. Lavor, N. Maculan, and A. Mucherino, “Euclidean distance geometry and applications,” *SIAM Review*, vol. 56, no. 1, pp. 3–69, 2014.
- [7] A. M.-C. So and Y. Ye, “Theory of semidefinite programming for Sensor Network Localization,” *Mathematical Programming*, vol. 109, no. 2-3, pp. 367–384, 2007.
- [8] J. Alencar, C. Lavor, and L. Liberti, “Realizing Euclidean distance matrices by sphere intersection,” *Discrete Applied Mathematics*, vol. 256, pp. 5–10, 2019.
- [9] M. Larsson, V. Larsson, K. Astrom, and M. Oskarsson, “Optimal Trilateration Is an Eigenvalue Problem,” in *IEEE ICASSP*, 2019, pp. 5586–5590.
- [10] A. Beck, P. Stoica, and J. Li, “Exact and Approximate Solutions of Source Localization Problems,” *IEEE Trans. Signal Process.*, vol. 56, no. 5, pp. 1770–1778, 2008.
- [11] T. Barfoot, C. Hay Tong, and S. Sarkka, “Batch Continuous-Time Trajectory Estimation as Exactly Sparse Gaussian Process Regression,” in *Robotics: Science and Systems*. Robotics: Science and Systems, 2014.
- [12] F. Caballero, L. Merino, and A. Ollero, “A General Gaussian-Mixture Approach for Range-only Mapping using Multiple Hypotheses,” in *IEEE ICRA*, 2010, pp. 4404–4409.
- [13] F. R. Fabresse, F. Caballero, I. Maza, and A. Ollero, “Undelayed 3D ROSLAM based on Gaussian-mixture and reduced spherical parametrization,” in *IEEE/RSJ IROS*, 2013, pp. 1555–1561.
- [14] J.-L. Blanco, J.-A. Fernandez-Madrigal, and J. Gonzalez, “Efficient probabilistic Range-Only SLAM,” in *IEEE/RSJ IROS*, 2008, pp. 1017–1022.
- [15] J.-L. Blanco, J. Gonzalez, and J.-A. Fernandez-Madrigal, “A pure probabilistic approach to range-only SLAM,” in *IEEE ICRA*, 2008, pp. 1436–1441.
- [16] T. D. Barfoot, *State Estimation for Robotics*. Cambridge University Press, 2017.
- [17] F. Dellaert and M. Kaess, “Square root SAM: Simultaneous localization and mapping via square root information smoothing,” *IJRR*, vol. 25, no. 12, pp. 1181–1203, 2006.
- [18] M. Kaess, H. Johannsson, R. Roberts, V. Ila, J. J. Leonard, and F. Dellaert, “iSAM2: Incremental smoothing and mapping using the Bayes tree,” *IJRR*, vol. 31, no. 2, pp. 216–235, 2012.
- [19] M. Pacholska, F. Dünmbgen, and A. Scholefield, “Relax and Recover : Guaranteed Range-Only Continuous Localization,” *IEEE RAL*, vol. 5, no. 2, pp. 2248–2255, 2020.
- [20] P. Furgale, T. D. Barfoot, and G. Sibley, “Continuous-Time Batch estimation Using Temporal Basis Functions,” in *IEEE ICRA*, 2012, pp. 2088–2095.
- [21] P. Biswas and Y. Ye, “Semidefinite programming for Ad Hoc Wireless Sensor Network Localization,” in *International Symposium on Information Processing in Sensor Networks*, 2004, pp. 46–54.
- [22] P. Biswas, T.-C. Lian, T.-C. Wang, and Y. Ye, “Semidefinite Programming Based Algorithms for Sensor Network Localization,” *ACM Transactions on Sensor Networks*, vol. 2, no. 2, pp. 188–220, 2006.
- [23] I. Dokmanić, R. Parhizkar, J. Ranieri, and M. Vetterli, “Euclidean Distance Matrices: Essential theory, algorithms, and applications,” *IEEE Signal Processing Magazine*, vol. 32, no. 6, pp. 12–30, 2015.
- [24] S. Boyd and L. Vandenberghe, *Convex Optimization*. Cambridge University Press, 2004.
- [25] L. Carbone, D. Rosen, G. Calafiore, J. Leonard, and F. Dellaert, “Lagrangian Duality in 3D SLAM: Verification Techniques and Optimal Solutions,” in *IEEE/RSJ IROS*, 2015.
- [26] L. Carbone and F. Dellaert, “Duality-based verification techniques for 2D SLAM,” in *IEEE ICRA*, 2015, pp. 4589–4596.
- [27] J. Fredriksson and C. Olsson, “Simultaneous Multiple Rotation Averaging Using Lagrangian Duality,” in *ACCV*, 2013, pp. 245–258.
- [28] J. Brialet and J. Gonzalez-Jimenez, “Fast global optimality verification in 3D SLAM,” in *IEEE/RSJ IROS*, 2016, pp. 4630–4636.
- [29] D. M. Rosen, L. Carbone, A. S. Bandeira, and J. J. Leonard, “SE-Sync: A certifiably correct algorithm for synchronization over the special Euclidean group,” *IJRR*, vol. 38, no. 2-3, pp. 95–125, 2019.
- [30] A. Eriksson, C. Olsson, F. Kahl, and T.-J. Chin, “Rotation Averaging and Strong Duality,” in *IEEE/CVF CVPR*, 2018, pp. 127–135.
- [31] F. Dellaert, D. M. Rosen, J. Wu, R. Mahony, and L. Carbone, “Shonan Rotation Averaging: Global Optimality by Surfing $\mathbb{SO}(p)$,” in *European Conference on Computer Vision*, 2020, pp. 292–308.
- [32] T. D. Barfoot, C. Holmes, and F. Dünmbgen, “A Fine Line: Total Least-Squares Line Fitting as QCQP Optimization,” *arXiv:2206.05082*, 2022.
- [33] H. Yang, P. Antonante, V. Tzoumas, and L. Carbone, “Graduated Non-Convexity for Robust Spatial Perception: From Non-Minimal Solvers to Global Outlier Rejection,” *IEEE RAL*, vol. 5, no. 2, pp. 1127–1134, 2020.
- [34] H. Yang, J. Shi, and L. Carbone, “TEASER : Fast and Certifiable Point Cloud Registration,” *IEEE Trans. Robot.*, vol. 32, no. 2, pp. 314–333, 2020.
- [35] D. Cifuentes, S. Agarwal, P. A. Parrilo, and R. R. Thomas, “On the local stability of semidefinite relaxations,” *Mathematical Programming*, no. 193, pp. 629–663, 2022.
- [36] G. H. Golub and C. F. Van Loan, *Matrix Computations*, 4th ed. The John Hopkins University Press, 2013.
- [37] L. Vandenberghe, “Chordal graphs and Semidefinite Optimization,” *Foundations and Trends in Optimization*, vol. 1, no. 4, pp. 241–433, 2015.
- [38] A. Goudar, W. Zhao, T. D. Barfoot, and A. P. Schoellig, “Gaussian Variational Inference with Covariance Constraints Applied to Range-Only Localization,” in *IEEE/RSJ IROS*, 2022.